

Table 4. Mean percentage value of the lymphocyte subset in the blood samples and various lymphoid tissues of normal guinea pigs by novel flow cytometry consisting of MIL4/SSC followed by FSC/SSC and specific antibody analysis^{a)}

		Mean	SD
Blood	T	54.2	10.7
	CD4 ⁺	26.6	9.9
	CD8 ⁺	16.1	12.1
	CD4-CD8-T	16.6	6.7
	B	45.7	11.8
	R27E	50.8	13.6
Spleen	T	56.1	4.3
	CD4 ⁺	26.4	4.1
	CD8 ⁺	22.8	6.6
	CD4-CD8-T	5.6	2.0
	B	43.1	4.4
	R27E	42.1	8.5
Thymus	T	94.0	2.6
	CD4 ⁺	6.5	3.1
	CD8 ⁺	11.2	6.2
	CD4 ⁺ CD8 ⁺	70.7	8.4
	CD4-CD8-T	8.8	3.7
	IgM (31D2)	1.5	0.6
	R27E	1.2	0.7
L.N	T	34.3	11.3
	CD4 ⁺	22.5	5.4
	CD8 ⁺	11.2	5.3
	CD4-CD8-T	<0.1	-
	B	59.1	10.3
	R27E	61.1	13.1

^{a)} Lymphocyte fraction was gated by the MIL4/SSC parameter, and each lymphocyte subset was studied by flow cytometry using the specific antibody shown in Table 1. The data are expressed as the mean ± SD. N=60.

lymphoid tissues and the blood has been similarly reported in humans and other rodents. The granulocyte fractions were 33.6 ± 14.2 and 3.1 ± 1.4% in blood and the spleen, respectively, and those in the thymus and LN were almost null. The MIL4-/SSC^{high} fractions containing Kurloff cells were 11.7 ± 6.5, 19.4 ± 7.3, 2.5 ± 0.8 and 1.8 ± 0.4% in the blood, spleen, thymus and LN, respectively, indicating that MIL4-/SSC^{high} Kurloff cells are mainly located in the spleen and blood of normal healthy guinea pigs (Table 3).

Detection of guinea pig-lymphocyte subsets in blood and various lymphoid tissues

The lymphocyte subsets of the guinea pigs were de-

termined by flow cytometry with three color staining using a consecutive flow cytometric procedure. The lymphocyte gating procedure initially used gating with MIL4/SSC, followed by gating with FSC/SSC (Fig. 1). The available antibodies against guinea pig-cell surface markers that are described in Table 1 were used to detect specific lymphocyte subsets and subpopulations (Table 4). Initially, the MHC Class II antigen expression on B-cells was verified with the staining of B (Msgp9) and MHC Class II (R27E) (data not shown). The mean percentage of T- and B-cells was 54.2 ± 10.7 and 45.7 ± 11.8% in the total lymphocytes of the blood samples, respectively.

The lymphocyte subsets of the CD4⁺ and CD8⁺ cells were 26.6 ± 9.9 and 16.1 ± 12.1% in the blood, 26.4 ± 4.1 and 22.8 ± 6.6% in the spleen, and 22.5 ± 5.4 and 11.2 ± 5.3% in LN, respectively, demonstrating that CD4⁺ lymphocytes were greater in number than the CD8⁺ lymphocytes in blood samples, the spleen and the lymph nodes. The thymocytes mostly expressed T-cell marker CT5 at a rate of 94.0 ± 2.6%, and CD4⁺CD8⁺ double positive cells were 70.7 ± 8.4%. However, membrane IgM⁺ thymocytes were negligible.

Since the accumulated percentage of CD4⁺ plus CD8⁺ lymphocytes was smaller than that of the pan-T-cells, we further analyzed the lymphocyte fraction by three color immunostaining for CD4 plus CD8 antigens vs. Pan-T-cell antigen (Fig. 2A). As expected, we identified the CD4-CD8⁻ T-cell population at 16.6 and 5.6% in the blood samples and the spleen, respectively. We then sorted the CD4-CD8⁻ T-cell population and a mixed population with the CD4⁺ plus CD8⁺ T-cell population. As shown in Figs. 2B and 2C, the CT7-CD8⁻ T-cells were bigger in size and richer in cytoplasm than those of CD4⁺ plus CD8⁺ T-cells as revealed by May-Giemsa staining. The mixed cell population with CD4⁺ plus CD8⁺ T-cells was homogeneous and was the so-called small lymphocyte that possesses a pyknotic nucleus and a narrow cytoplasm. Furthermore, approximately 40% of the CD4-CD8⁻ T-cell subpopulation was positive for asialo GM1 (Figs. 2D and 2E).

Comparison of percentage positives of lymphocyte subsets between the adult and newborn guinea pigs

The mean percentage for T, B, CD4⁺ CD8⁺ and CD4-CD8⁻ T-cells were compared between adult and newborn guinea pigs at the ages of 2 years old (N=12)

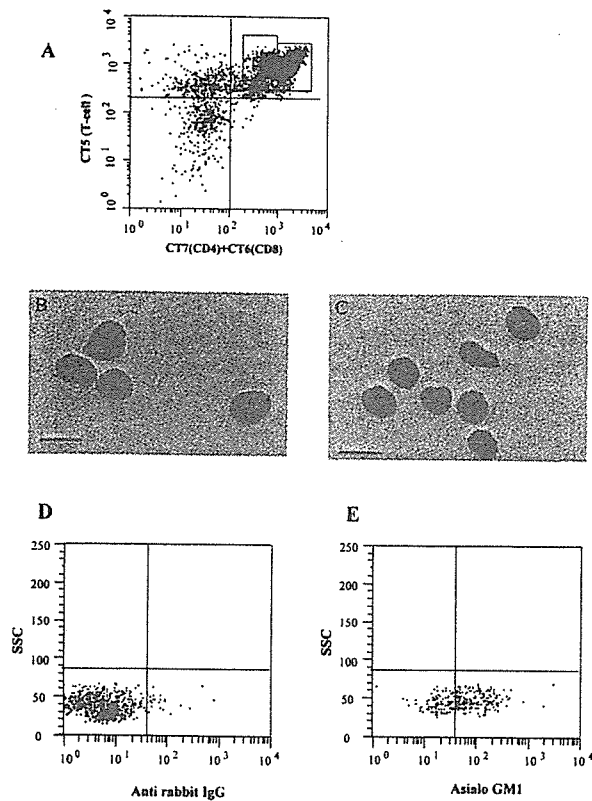


Fig. 2. Detection of a CD4-CD8⁻ T-cell subset and its morphological characterization. (A) The population of CD4-CD8⁻ T-cells was detected by flow cytometry using three color staining of the lymphocyte fraction with FITC-CT6, FITC-CT7 and PE-CT5. Dead cells were removed by propidium iodide, and viable cells were analyzed. The CD4^{high}CD8^{high} and CD4⁺CD8⁺ subpopulations represent CD8⁺ and CD4⁺ T-cell subsets, respectively. B and C: Light-microscopic analysis of CD4-CD8⁻ (B) and CD4⁺CD8⁺ T-cells (C) by May-Giemsa staining. The lymphocyte subpopulation was purified by flow cytometric sorting from normal guinea pig blood. Detection of asialo GM1⁺ cells in the CD4-CD8⁻ T-cell subpopulation. The asialo GM1⁺ cell subpopulation was detected by four color staining. Dead cells were removed by propidium iodide and remaining viable cells were analyzed. Lymphocyte population was initially gated with FSC/SSC followed by gating with CT5/CT7 and CT6 for detecting the CD4-CD8⁻ T-cell subpopulation. Then, gating with SSC/anti-rabbit IgG was used as reference for the gating (D), and asialo GM1⁺ cells in CD4-CD8⁻ T-cell subpopulation were detected by gating with SSC/anti-asialo GM1 rabbit antibody followed by PE-anti-rabbit IgG (E).

and 3 days old (N=12) (Fig. 3). The newborn animals were significantly lower in CD8⁺ lymphocytes at a percentage of 10.2 ± 2.7 than the adult animals ($17.4 \pm 5.6\%$, $P < 0.01$). On the other hand, the newborn ani-

mals had a significantly higher percentage of CD4-CD8⁻ T-cells, at 25.4 ± 10.1 , than the adults with $15.5 \pm 4.3\%$ ($P < 0.05$). The other subsets of the T, B and CD4⁺ lymphocyte rates did not differ between the two groups.

Appearance of MHC Class II⁺ T-cell subset in the blood after intravenous inoculation of a large amount of BCG

We studied the effect of BCG inoculation on the percentage change in lymphocyte subsets using the procedure established above. By intravenous inoculation of 5 mg of BCG-Tokyo vaccine strain, the immunized animals expressed MHC Class II antigen on approximately 30% of the T-cells in the spleen at 6 weeks post-inoculation (Fig. 4A). In contrast, spleen cells from non-immunized animals or animals immunized with 0.1 mg of BCG intradermally showed no MHC Class II⁺ T-cells (Fig. 4B), suggesting that expression of MHC Class II antigen on T-cells may be a marker of hyper-activation of T-lymphocytes in animals inoculated with a large amount of BCG.

Discussion

The guinea pig has been used as model animal to study various infectious diseases, allergies and tumors, and it has been especially used for the study of BCG and *Mycobacterium tuberculosis*. However, guinea pigs have limitations for immunological study because of a lack of immunological procedures and reagents compared with mice.

In this study, we established flow cytometric procedures enabling differentiation between guinea pig leukocyte fractions and lymphocyte subsets. Applying anti-MIL4 antibody, which recognizes porcine neutrophils, eosinophils and basophils [9], and was cross-reacted with guinea pig granulocyte and monocytes, and SSC to gate the leukocyte fractions, the mean percentages of the lymphocyte and granulocyte fractions in the blood were 48.7 ± 14.1 and $33.6 \pm 14.2\%$. In humans, blood lymphocytes and granulocytes are 40 ± 13 and $53 \pm 17\%$ [20]. On the other hand the mean values of lymphocytes and granulocytes were reported as 81 ± 10 and $15 \pm 11\%$ in mice, 70 ± 13 and $24 \pm 18\%$ in rats, and 73 ± 19 and $22 \pm 5\%$ in hamsters [20]. Thus, other rodents show a higher percentage of lymphocytes and a lower percentage of granulocytes than

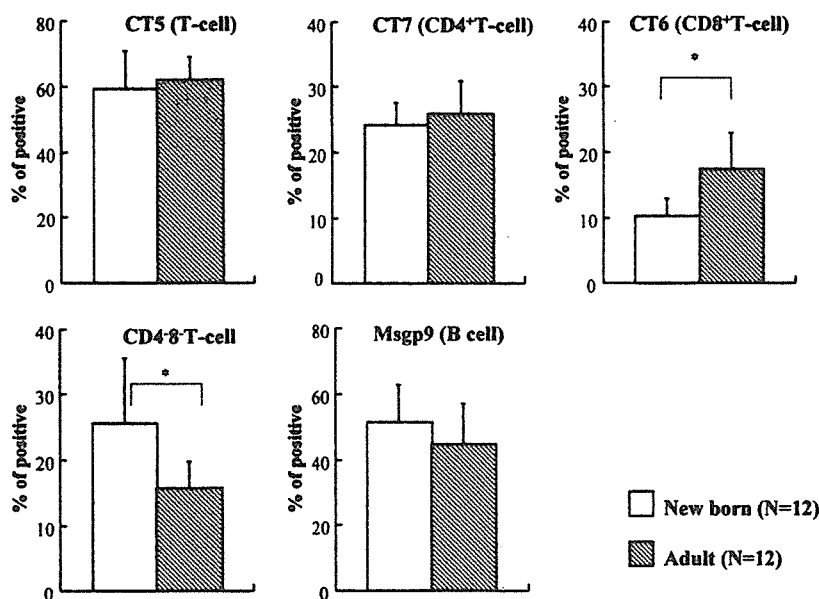


Fig. 3. Comparison of percentages of lymphocyte subsets between adult and newborn guinea pigs. The open column shows the mean results from newborn guinea pigs between 3 to 11 days, and the hatched column shows the mean results from adult guinea pigs aged 2 years. The data are expressed as the mean \pm SD. *, $P < 0.05$ significant difference between the two groups of guinea pigs.

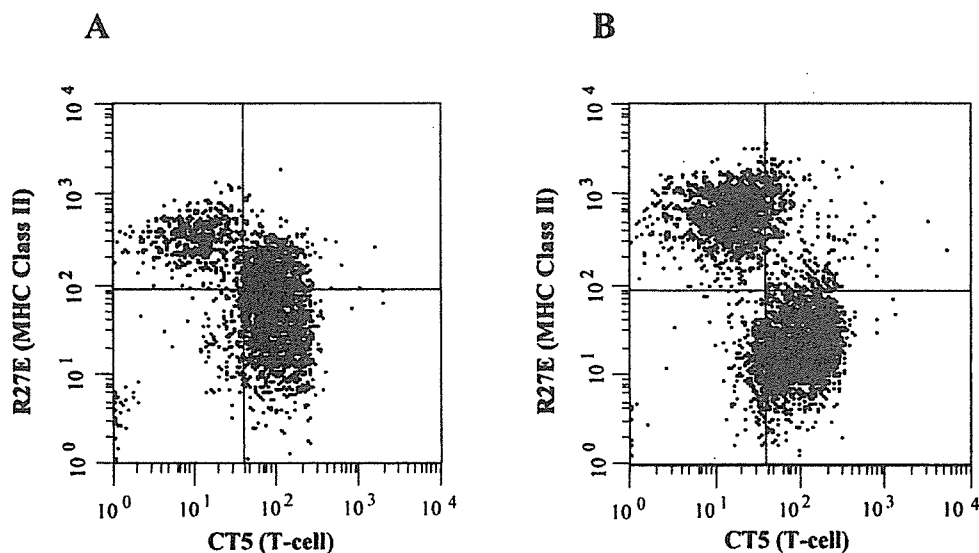


Fig. 4. An MHC Class II⁺ T-cell subpopulation appeared in the spleen at 6 weeks post-intravenous inoculation with large amounts of BCG. Dead cells were removed by propidium iodide, and viable cells of the lymphocyte gate were analyzed. (A) Appearance of the unique MHC Class II⁺ T-cell subpopulation in animals inoculated with a high dose of BCG intravenously. (B) MHC Class II⁺ T-cell subpopulation in normal control animals was not detected.

those of guinea pigs. Are there any differences in the leukocyte fractions obtained by the different methods of morphological analysis by other researchers and our

flow cytometry using MIL4/SSC parameter? In the study of human leukocyte fractions, human CD45/SSC gating separated the leukocyte fractions consisting of

lymphocytes, monocytes and granulocytes. Moreover, the flow cytometric procedure obtained an identical count for each leukocyte [16]. These results suggest that the mean values of each leukocyte fraction of the guinea pigs are more similar to those of humans than those of other rodents.

Interestingly, DTH induction and hormone physiology in BCG-immunized guinea pigs are reported to be more similar to those of humans than other rodents [13, 18, 27]. Recently, molecular analysis has revealed that the CD1 gene family of the guinea pig is much more similar to humans than mice and other rodents [3, 11, 12]. Thus, the guinea pig should be a better model animal because of the resemblance of immunity, hormone physiology and genetic background against pathogens to those of humans.

Comparing lymphocyte subsets between newborn and adult animals, the CD8⁺ T-cell subsets in newborn animals were significantly lower than those of adult animals, while the CD4⁺CD8⁻ T-cell subset was higher than that of the adult group. The T-cell fraction rate in the total leukocytes between both groups was similar. Although the increase in the CD8⁺ T-cell rate in proportion to age seems reasonable, the presence of the CD4⁺CD8⁻ T-cell subset and the decrease in the rate in the elderly population is not well understood. The CD4⁺CD8⁻ T-cells were bigger in size than the CD4⁺ or CD8⁺ T-cells, and possessed abundant cytoplasm. More than half of the cell population was positive for asialo GM1, suggesting that this unique T-cell subset might function as NK or CTL. Further study on these functions is required to clarify this subpopulation.

The present flow cytometric procedure is a useful tool for studying T-cell subsets and subpopulations. Intravenous inoculation with a high dose of BCG specifically induced MHC Class II⁺ T-cells in inoculated guinea pigs, whereas it was not detected in immunized animals intradermally inoculated with the common dose of BCG or in normal healthy control animals. Although these results suggest that the expression of MHC Class II antigen on T-cells may be related to T-cell activation due to BCG infection, the appearance of the MHC Class II⁺ T-cells is probably related to the hyper-activation of T-cells, because the common dose of BCG vaccination did trigger the induction of the antigen specific immune-competent T-cells in the immunized animals. Our results of in-

duction of MHC Class II⁺ T-cells in guinea pigs inoculated with a high dose of BCG seem to be partly explained by a report by Zhou *et al.* [34] in which intravenous inoculation with a high dose BCG enhanced the pathogenicity of immunodeficiency virus infection.

Previously, other researchers reported that the mean value of the leukocyte count in guinea pigs was 10,830, 12,000, 8,280, 10,000 and 9,000/ μ l using the hemacytometer chamber [23], which is significantly higher than our result of 5,438/ μ l detected by the automated blood analyzer. We speculate that these differences are not due to the two different procedures of the cell counting using the hemacytometer chamber and automated blood analyzer, but are mainly due to differences in the environmental factors of raising and feeding animals, because blood cell counts of the guinea pigs by the two different procedures were identical as described in Materials and Methods. Thus, novel procedures for analysis of cell count, leukocyte fractions and lymphocyte subsets and subpopulations in the blood and lymphoid tissues, and their established normal values in this study, will provide an effective tool for studying the guinea pig as a model animal.

Acknowledgments

The Japan Health Science Foundation and the Japanese Ministry of Health, Labor and Welfare supported this work. This study was also supported by the AIDS vaccine project in conjunction with the Japan Science and Technology Cooperation.

References

1. Baldwin, S.L., D'Souza, C., Roberts, A.D., Kelly, B.P., Frank, A.A., Lui, M.A., Ulmer, J.B., Huygen, K., McMurray, D. M., and Orme, I.M. 1998. Evaluation of new vaccines in the mouse and guinea pig model of tuberculosis. *Infect. Immun.* 66: 2951-2959.
2. Bersani-Amado, C.A., Duarte, A.J.S., Tanji, M.M., Cianga, M., and Jancar, S. 1990. Comparative study of adjuvant induced arthritis in susceptible and resistant strains of rats. III. Analysis of lymphocyte subpopulations. *J. Rheumatol.* 17: 153-158.
3. Dascher, C.C., Hiromatsu, K., Naylor, J.W., Brauer, P.P., Brown, K.A., Storey, J.R., Behar, S.M., Kawasaki, E.S., Porcelli, S.A., Brenner, M.B., and LeClair, K.P. 1999. Conservation of a CD1 multigene family in the guinea pig. *J. Immunol.* 163: 5478-5488.
4. Emery, P., Gentry, K.C., Mackay, I.R., Muirden, K.D.,

- and Rowley, M. 1987. Deficiency of the suppressor inducer subset of T lymphocytes in rheumatoid arthritis. *Arthritis Rheum.* 30: 849–856.
5. Epstein, J.H. 1992. Experimental models for primary melanoma. *Photodermatol. Photoimmunol. Photomed.* 9: 91–98.
 6. Eremin, O., Coombs, R.R., Ashby, J., and Plumb, D. 1980. Natural cytotoxicity in the guinea-pig: the natural killer (NK) cell activity of the Kurloff cell. *Immunology* 41: 367–378.
 7. Evans, E.F., Wilson, J.P., and Borerwe, T.A. 1981. Animal models of tinnitus. *Ciba Found. Symp.* 85: 108–138.
 8. Giebink, G.S. 1999. Otitis media: the chinchilla model. *Microb. Drug Resist.* 5: 57–72.
 9. Haverson, K., Bailey, M., Higgins, V.R., Bland, P.W., and Stokes, C.R. 1994. Characterization of monoclonal antibodies specific for monocytes, macrophages and granulocytes from porcine peripheral blood and mucosal tissues. *J. Immunol. Methods* 170: 233–245.
 10. Helm, R.M. 2002. Food allergy animal models. An overview. *Ann. N.Y. Acad. Sci.* 964: 139–150.
 11. Hiromatsu, K., Dascher, C.C., LeClair, K.P., Sugita, M., Furlong, S.T., Brenner, M.B., and Porcelli, S.A. 2002. Induction of CD1-restricted immune responses in guinea pigs by immunization with mycobacterial lipid antigens. *J. Immunol.* 169: 330–339.
 12. Hiromatsu, K., Dascher, C.C., Sugita, M., Gingrich-Baker, C., Behar, S.M., LeClair, K.P., Brenner, M.B., and Porcelli, S.A. 2002. Characterization of guinea-pig group 1 CD1 proteins. *Immunology* 106: 159–172.
 13. Jonsson, E.W. 1998. Functional characterization of receptors for cysteinyl leukotrienes in smooth muscle. *Acta. Physical. Scand. Suppl.* 641: 1–55.
 14. Kasai, M., Iwamori, M., Nagai, Y., Okumura, K., and Tada, T. 1980. A glycolipid on the surface of mouse natural killer cells. *Eur. J. Immunol.* 10: 175–180.
 15. Koch, R. 1982. Classics in infectious disease. The etiology of tuberculosis: Robert Koch. Berlin, Germany. *Rev. Infect. Dis.* 4: 1270–1274.
 16. Lacombe, F., Durrieu, F., Briais, A., Dumain, P., Belloc, F., Bascans, E., Reiffers, J., Boisseau, M.R., and Bernard, P. 1997. Flow cytometry CD45 gating for immunophenotyping of acute myeloid leukemia. *Leukemia* 11: 1878–1886.
 17. Landmore, G., Debout, C., Quillec, M., and Izard, J. 1984. Isolation of Kurloff cells by Percoll density gradient centrifugation. Protein labeling with ³⁵S-methionine of these cells. *Biol. Cell.* 50: 121–126.
 18. Lechner, A.J. and Bancho, N. 1982. Advanced pulmonary development in newborn guinea pigs (*Cavia porcellus*). *Am. J. Anat.* 163: 235–246.
 19. Miller, H.I. and Parker, J.L. 1989. The guinea pig as a model in shock research. *Prog. Clin. Biol. Res.* 299: 277–286.
 20. Mitruka, B.M. and Rawnley, H.M. 1981. The collection of reference value of blood and clinical chemistry of experimental animal and human. *In: Experimental animal and human hematology.* Seishi Shoin, Tokyo.
 21. Ogura, A., Noguchi, Y., Yamamoto, Y., Shibata, S., Asano, T., Okamoto, Y., and Honda, M. 1996. Localization of HIV-1 in human thymic implant in SCID-hu mice after intravenous inoculation. *Int. J. Exp. Pathol.* 77: 201–206.
 22. Rapp, H.J. 1973. A guinea pig model for tumor immunology. A summary. *Isr. J. Med. Sci.* 9: 366–374.
 23. Siegmund, S. 1967. The Blood Morphology of Laboratory Animal 3. F. A. Davis Company, Philadelphia.
 24. Steerenberg, P.A., De Jong, W.H., Geerse, E., De Graaf, A., Scheper, R.J., Den Otter, W., and Ruitenber, E.J. 1991. Major histocompatibility complex class II antigen expression on leukocyte subpopulations in the draining lymph node and tumor in the early phase of bacillus-Calmette-Guerin-induced tumor regression. *Cancer Immunol. Immunother.* 33: 189–197.
 25. Summerfield, A., Haverson, K., Thacker, E., and McCullough, K.C. 2001. Differentiation of porcine myeloid bone marrow haematopoietic cell populations. *Vet. Immunol. Immunopathol.* 80: 121–129.
 26. Takizawa, M., Chiba, J., Haga, S., Asano, T., Yamamoto, N., and Honda, M. 2003. Fraction of guinea pig leukocyte by flow cytometry using a novel MIL4/SSC parameter. *Cytometry Research* 13: 25–32.
 27. Tallarida, R.J. 1988. Pharmacologic methods for identification of receptors. *Life Sci* 43: 2169–2176.
 28. Tan, B.T., Ekelaar, F., Luirink, J., Rimmelzwaan, G., De Jonge, A.J., and Scheper, R.J. 1985. Production of monoclonal antibodies defining guinea pig T-cell surface markers and a strain 13 Ia-like antigen: the value of immunohistological screening. *Hybridoma.* Summer 4: 115–124.
 29. Verdier, F., Chazal, I., and Descotes, J. 1994. Anaphylaxis models in the guinea pig. *Toxicology* 93: 55–61.
 30. Wicher, K., and Wicher, V. 1989. Experimental syphilis in guinea pig. *Crit. Rev. Microbiol.* 16: 181–234.
 31. Wicher, V. and Wicher, K. 2001. Pathogenesis of maternal-fetal syphilis revisited. *Clin. Infect. Dis.* 33: 354–363.
 32. Yoshino, N., Ami, Y., Terao, K., Tashiro, F., and Honda, M. 2001. Upgrading of flow cytometric analysis for absolute counts, cytokines and other antigenic molecules of cynomolgus monkeys (*Macaca fascicularis*) by using and-human cross-reactive antibodies. *Exp. Anim.* 49: 97–110.
 33. Yoshino, N., Ryu, T., Sugamata, M., Ihara, T., Ami, Y., Shinohara, K., Tashiro, F., and Honda, M. 2000. Direct detection of apoptotic cells in peripheral blood from highly pathogenic SHIV-inoculated monkey. *Biochem. Biophys. Res. Commun.* 263: 868–874.
 34. Zhou, D., Shen, Y., Chalifoux, L., Lee-Parritz, D., Simon, M., Sehgal, P.K., Zheng, L., Halloran, M., and Chen, Z.W. 1999. *Mycobacterium bovis* Bacille Calmette-Guerin enhances pathogenicity of simian immunodeficiency virus infection and accelerates progression to AIDS in macaques: a role of persistent T cell activation in AIDS pathogenesis. *J. Immunol.* 162: 2204–2216.

Alternatively spliced transcripts of Fas mRNAs in feline lymphoid cells

T. Mizuno, K. Baba, Y. Goto, K. Masuda, K. Ohno & H. Tsujimoto

Summary

Fas belongs to the tumour necrosis factor receptor family and transduces the death signal after binding to the Fas ligand. Five feline lymphoma cell lines were shown, by reverse transcription-polymerase chain reaction, to express six species of Fas transcripts. Based on sequence comparison of these Fas transcripts with the genomic Fas gene, five of the six transcripts were found to be generated through alternative splicing and to encode five different Fas proteins lacking the transmembrane domain. We also detected such alternatively spliced transcripts in primary tumour tissues from cats with naturally occurring lymphoma. These results suggest a possible association of the alternatively spliced Fas variants with the pathogenesis of feline lymphoma.

Introduction

Fas is a cell-surface receptor of type I membrane proteins belonging to the nerve growth factor (NGF) receptor/tumour necrosis factor (TNF) receptor superfamily (Itoh *et al.*, 1991). Fas induces apoptosis after binding to the Fas ligand or anti-Fas agonistic immunoglobulin. Fas consists of three domains: the extracellular domain; the transmembrane domain; and the cytoplasmic domain. The cytoplasmic domain contains a death domain essential for transduction of the death signal.

Human Fas is expressed in a wide variety of tissues and cells, such as the normal thymus, liver, heart and kidney, as well as malignant tumour cells (Nagata 1997). Authentic human Fas is a membrane-anchored protein, whereas its soluble form, lacking the transmembrane domain, blocks apoptosis induced by anti-Fas immunoglobulin (Cheng *et al.*, 1994). Cascino *et al.* (1995) reported two other Fas mRNA species in activated human peripheral blood mononuclear cells (PBMcs) and human tumour cell lines, in addition to the soluble form. These Fas mRNA variants were shown to have frameshifts that generate

premature termination codons and encode soluble proteins blocking the anti-Fas antibody-induced cell death.

It was recently reported that the amount of soluble Fas was increased in the sera of humans with various diseases, such as autoimmune diseases, including systemic lupus erythematosus (SLE) (Cheng *et al.*, 1994) and rheumatoid arthritis (RA) (Hasunuma *et al.*, 1997), and malignancies, including lymphoma (Yufu *et al.*, 1998; Niitsu *et al.*, 1999; Hara *et al.*, 2000), adult T-cell leukaemia (Sugahara *et al.*, 1997; Kamihira *et al.*, 1999), acute myeloid leukaemia (Inaba *et al.*, 1999), breast cancer (Kimura *et al.*, 1999; Ueno *et al.*, 1999), bladder cancer (Mizutani *et al.*, 1998) and gastric cancer (Lee *et al.*, 1998). In these disorders, the soluble Fas is considered to block the binding of Fas ligand to Fas, which may be one of the mechanisms used for the escape from cytotoxic T lymphocytes.

Previously, we cloned feline Fas cDNA (Mizuno *et al.*, 1998), but there has been no report on the variant transcript of the feline Fas gene. In the present study, we detected five species of Fas mRNAs, of different sizes, in feline lymphoid cells and characterized them in comparison to the genomic sequence of the feline Fas gene.

Materials and methods

Cell cultures

Five feline lymphoid tumour cell lines — FT-1 (Miura *et al.*, 1987; 1989), FL-74 (Theilen *et al.*, 1969), F422 (Rickard *et al.*, 1969), 3201 (Snyder *et al.*, 1978) and MCC (Cheney *et al.*, 1990) — were cultured (at 37 °C in a humidified atmosphere of 5% CO₂ in air) in RPMI-1640 supplemented with 10% heat-inactivated fetal calf serum (FCS) and antibiotics. FT-1, FL74 and F422 cell lines were derived from lymphomas in cats infected with feline leukaemia virus (FeLV), whereas 3201 and MCC cell lines were negative for FeLV.

PBMcs were separated by the Ficoll-Hypaque density-gradient centrifugation of peripheral blood samples from two specific pathogen-free cats. The cells were resuspended in RPMI-1640 supplemented with 10% FCS, antibiotics, 100 U mL⁻¹ recombinant human interleukin-2 (IL-2) and 10 µM 2-mercaptoethanol. The resultant PBMcs were cultured in the presence of concanavalin A (Con A) (5 µg mL⁻¹) (Sigma Chemical Co., St Louis, MO) in a six-well plate at 37 °C for 3 d. The cells were then pelleted by centrifugation, frozen in liquid nitrogen and stored at -80 °C for subsequent RNA isolation.

Department of Veterinary Internal Medicine, Graduate School of Agricultural and Life Sciences, The University of Tokyo, 1-1-1 Yayoi, Bunkyo-ku, Tokyo 113-8657, Japan

Received 2 October 2002; accepted 11 November 2002

Correspondence: Koichi Ohno, Department of Veterinary Internal Medicine, Graduate School of Agricultural and Life Sciences, The University of Tokyo, 1-1-1 Yayoi, Bunkyo-ku, Tokyo 113-8657, Japan. E-mail: aohno@mail.ecc.u-tokyo.ac.jp

Primer name	Sequence	Nucleotide position	PCR product
6S	5'-GGC GGG GCG CTC CGC AGC C-3'	-19-1	360 bp
6R	5'-TTC TAA GCC ATG CTT TCA T-3'	322-341	
7S	5'-GAA GAA GCG AAG GAC TAC ACA GAC-3'	255-278	442 bp
7R	5'-GTT CGG CAA TGC TAC TGA TG-3'	677-696	
8S	5'-GAA TCT ACA GTC TCA GTT AC-3'	619-631	354 bp
8R	5'-GCA GTT TCC ATT CTC AAG-3'	945-972	

Table 1. Primer pairs used for reverse transcription-polymerase chain reaction (RT-PCR) of feline Fas

Primary tumour tissues

Specimens of tumour tissues were obtained from 11 cats with lymphoma referred to the Veterinary Medical Center of the University of Tokyo for diagnosis and treatment. The tumour tissues obtained at biopsy or necropsy were rapidly frozen in liquid nitrogen and stored at -80°C for subsequent RNA extraction.

Reverse transcription-polymerase chain reaction (RT-PCR)

Total RNA was extracted from the cells and tissues by acid guanidium-phenol-chloroform with RNazol (Bio-tec, Houston, TX). After removal of contaminating DNA by treatment with DNase I (Life Technologies, Rockville, MD), cDNA was generated from 0.5 μg of total RNA using an RNA PCR core kit (Perkin Elmer Applied Biosystems, Foster City, CA) according to the manufacturer's protocol. Oligo dT primer was used to prime the first-strand cDNA synthesis for each of the reactions. Three primer pairs (6S/6R, 7S/7R and 8S/8R) were synthesized, based on the sequence of feline Fas cDNA (Mizuno *et al.*, 1998), to amplify the full-length coding region of feline Fas (Table 1). The PCR reaction consisted

of 40 cycles of denaturation at 94°C for 1 min and annealing/polymerization at 60°C for 1 min, followed by a final extension at 72°C for 7 min. These amplified products were electrophoretically separated through a 12.5% acrylamide gel and visualized by silver staining using a GenePhor electrophoresis unit (Amersham Pharmacia Biotech, Bucks., UK).

Nucleotide sequence determination of the PCR products

The PCR products were gel purified and subcloned into the pGEM-T Easy vector (Promega, Madison, WI). At least four clones from each of the differently sized PCR bands were sequenced by the dideoxy chain-termination reaction using a 377 Genetic Analyser (Perkin Elmer Applied Biosystems).

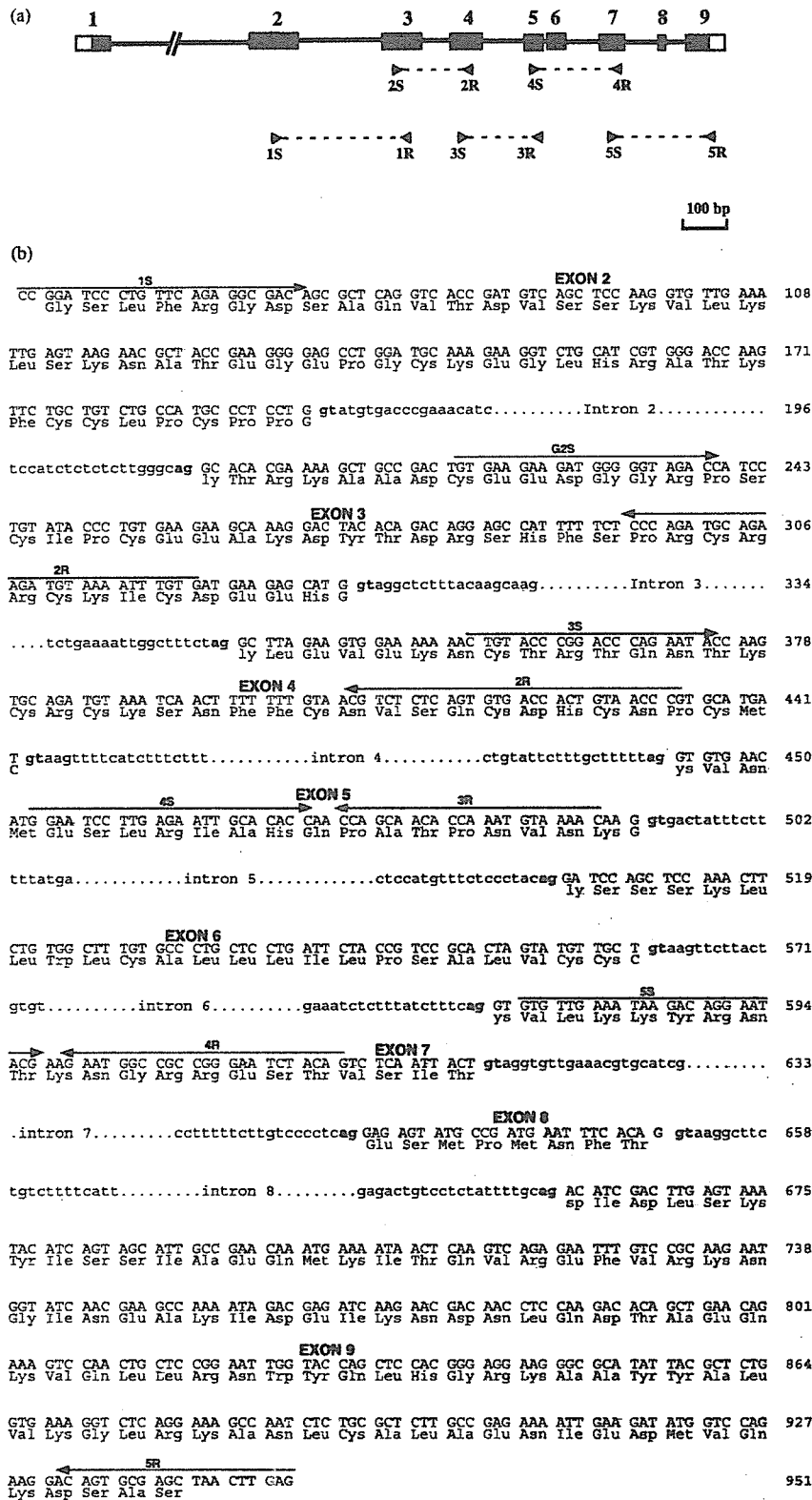
Cloning and sequencing of genomic DNA

Genomic DNA (500 ng), extracted from normal cat spleen, was amplified using an LA-PCR kit (Takara, Kyoto, Japan). Primer pairs used for PCR cloning of the feline genomic Fas gene were 1S/1R, 2S/2R, 3S/3R, 4S/4R and 5S/5R (Table 2, Fig. 1a & b). Sequences of the primers were based on the previously reported sequence of feline Fas

Table 2. Primer pairs used for genomic polymerase chain reaction (PCR) of feline Fas

Primer name	Sequence	Nucleotide position	Corresponding exon
1S	5'-CCG GAT CCC TGT TCA GAG GCG ACA-3'	47-70	2
1R	5'-CAC AAA TTT TAC ATC TTC TGC ATC TGG G-3'	295-322	3
2S	5'-GTG AAG AAG ATG GGG GTA GAC C-3'	218-239	3
2R	5'-CGG GTT ACA GTG GTC ACA CTG AGA GAC G-3'	408-435	4
3S	5'-CTG TAC CCG GAC CCA GAA TAC-3'	354-374	4
3R	5'-GTT TAC ATT TGG TGT TGC TGG-3'	478-499	5
4S	5'-GGA ATC CTT GAG AAT TGC ACA CC-3'	454-476	5
4R	5'-CTG TAG ATT CCC GGC GGC CAT TC-3'	600-622	7
5S	5'-GTG TTG AAA AAG TAC GGG AAT ACG-3'	572-592	7
5R	5'-CTC AAG TTA GCT CGC ACT GT-3'	967-986	9

Figure 1. Structure of the feline genomic Fas gene. (a) Exon/intron organization of the feline genomic Fas gene. Exons are represented by boxes and putatively numbered from the sequence alignment of the feline Fas gene and with the homologues of other species. Introns are represented by horizontal lines. Coding sequences in the exons are shown as filled boxes. Locations of the primers for cloning of the feline genomic Fas gene are indicated by arrowheads. (b) Nucleotide and predicted amino acid sequences of the feline genomic Fas gene. Nucleotides at the intron/exon boundaries are shown in bold type. Nucleotide numbering was based on the sequence of feline Fas cDNA previously reported (Mizuno *et al.*, 1998). Amino acids are numbered from the first methionine. Primers used for genomic polymerase chain reaction (PCR) are indicated by arrows.



cDNA (Mizuno *et al.*, 1998). The PCR products were cloned into the pGEM-T Easy vector and sequenced using a 377 Genetic Analyser (Perkin Elmer Applied Biosystems).

Results

Genomic organization of the feline Fas gene

Based on the sequence of feline Fas cDNA, to identify the genomic organization of the feline Fas gene a feline genomic DNA sample was subjected to PCR to amplify the introns and determine the exon/intron boundaries. A fragment amplified using primers 1S and 1R contained a region of the Fas gene corresponding to exons 2–3. Similarly, four more fragments corresponding to exons 3–4 (2S/2R), exons 4–5 (3S/3R), exons 5–7 (4S/4R), and exons 7–9 (5S/5R) were cloned. The exons of the feline genomic Fas gene were putatively numbered from the exon numbers of Fas genes of other species previously reported (Behrmann *et al.*, 1994; Cheng *et al.*, 1995; Yoo *et al.*, 1996). Sequences of the amplified DNA fragments were determined and compared with that of feline Fas cDNA reported previously (Mizuno *et al.*, 1998). All of the exon/intron boundaries in the cloned genomic Fas gene were consistent with the established GT/AG rule for splicing (Breathnach *et al.*, 1978) (Fig. 1a & b). The genomic organization of the exons and introns of the feline Fas gene was apparently the same as those of Fas genes of other species, including humans (Behrmann *et al.*, 1994; Cheng *et al.*, 1995) and cattle (Yoo *et al.*, 1996), reported previously.

Identification and characterization of Fas mRNA variants in feline lymphoid tumour cell lines

To characterize feline Fas mRNA, RNA samples from five feline lymphoma cell lines were analysed by RT-PCR. We carried out a series of RT-PCR amplifications by using specific primers to amplify three overlapping fragments of feline Fas mRNA (Table 1 and Fig. 3). By using two sets of primers (6S/6R and 8S/8R), PCR products of 360 bp and 354 bp, respectively, were amplified. The sizes of these fragments were the same as those expected from the sequence of authentic feline Fas cDNA reported previously (Mizuno *et al.*, 1998). RT-PCR, using another primer pair (7S/7R) encompassing exons 3–7, generated four or five bands of different sizes in all of the five feline lymphoma cell lines used in this study (Fig. 2a). In addition to a fragment of 442 bp corresponding to the authentic Fas mRNA (band A), five other fragments, of smaller sizes, were observed (bands B, C, D, E and F) (Fig. 2a). Band A, derived from the authentic Fas transcript, was the most intense. Bands B and D were distinct in all five cell lines but were less intense than band A. Band C was very faint in all cell lines. Bands E and F were slightly less intense than bands B and D, and band F was not detected in one (MCC) of the five cell lines.

Nucleotide sequences of the five bands B, C, D, E and F were compared with that of a band derived from the

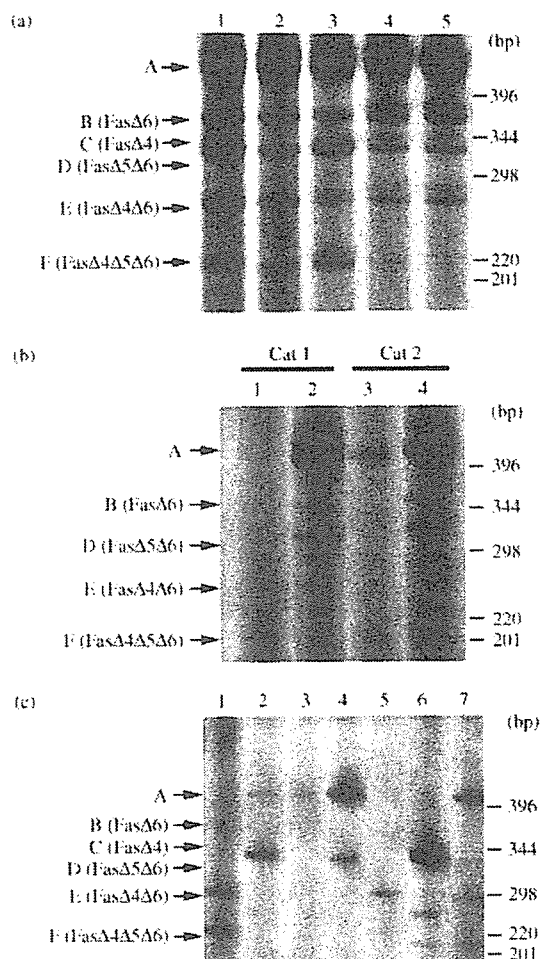


Figure 2. Reverse transcription–polymerase chain reaction (RT-PCR) analysis for Fas transcripts in feline lymphoid cell lines (a), concanavalin A (Con A)-activated feline peripheral blood mononuclear cells (PBMCs) (b), and primary tumour tissues from cats with lymphoma (c). Total RNA was extracted from the feline lymphoma cell lines, FT-1 (lane 1), FL-74 (lane 2), F422 (lane 3), 3201 (lane 4) and MCC (lane 5) (a), from unstimulated PBMCs (lanes 1 and 3) and Con A-stimulated PBMC (lanes 2 and 4) (b), and from primary tumour tissues (lane numbers indicate cat numbers) (c), and were subjected to RT-PCR analysis. The RNA samples were amplified by RT-PCR with primers 7S/7R. The PCR products were separated through a 12.5% polyacrylamide gel.

authentic feline Fas mRNA (band A) (Fig. 3a & b). Band B was shown to be derived from an mRNA species with a deletion of 69 bp corresponding to exon 6 (Fas Δ 6). The deletion found in the Fas Δ 6 mRNA did not generate a frameshift, and the Fas Δ 6 was shown to encode a smaller protein lacking its transmembrane domain. Nucleotide sequencing of band C revealed a deletion of 110 bp, corresponding to exon 4 (Fas Δ 4), a frameshift from the beginning of exon 5 and the generation of a premature termination codon at nucleotide position 544 in exon 6. Band D was shown to lack a fragment of 127 bp, which

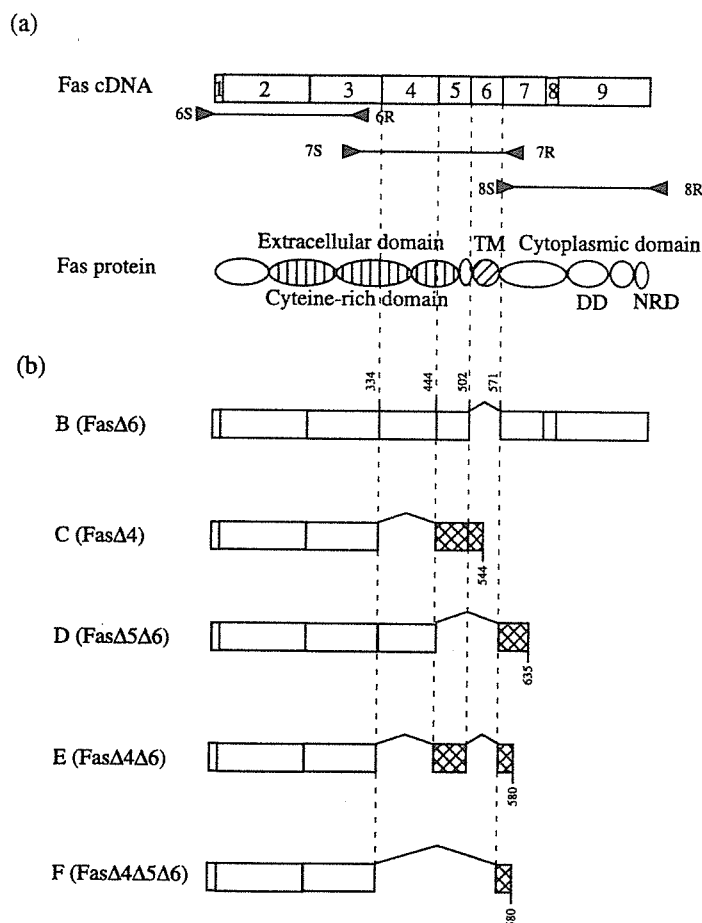


Figure 3. Schematic representation of normal and variant feline Fas mRNAs. (a) Nine exons encoding feline Fas are shown. TM, DD and NRD indicate the transmembrane domain, death domain and negative regulatory domain, respectively. (b) Structures of variant Fas mRNAs. Regions lacking in Fas mRNA variants are indicated by broken lines. The coding regions are shown in boxes. Cross-hatched boxes indicate exons with frameshifts.

encompassed exons 5 and 6 (Fas Δ 5 Δ 6) and to generate a frameshift and a premature stop codon at nucleotide position 577 in exon 7. Lack of exons 4 and 6 was found in the band E sequence (Fas Δ 4 Δ 6), generating a frameshift of exons 5 and 7 and a termination codon at nucleotide position 577 in exon 7. In the sequence of the smallest band F, exons 4, 5 and 6 were shown to be deleted (Fas Δ 4 Δ 5 Δ 6), generating a frameshift of exon 7 and a premature stop codon at nucleotide position 634. All of the sequences from the splicing variants were submitted to GenBank (GenBank accession nos: AB072009, AB072010, AB072011, AB072012, AB072013 and AB072014).

Detection of Fas mRNA variants in Con A-activated normal PBMC

RT-PCR analysis indicated that expression of Fas mRNA was increased in normal feline PBMCs after stimulation with Con A. To establish the presence of the alternatively spliced transcripts of Fas mRNA in the activated PBMCs, the Con A-activated PBMCs from two normal cats were subjected to RT-PCR analysis for Fas mRNA. RT-PCR analysis of Con A-activated feline PBMCs with two

primers pairs (6S/6R and 8S/8R) gave bands of 360 bp and 354 bp, respectively, which coincided with the size of bands derived from normal feline Fas mRNA. Nevertheless, RT-PCR with a different primer pair, 7S/7R, generated three to four bands in addition to the most intense band corresponding to the authentic Fas transcript (Fig. 2b).

Nucleotide sequencing of these DNA fragments showed that the four fragments detected in the PBMCs from cat 1 corresponded to Fas Δ 6, Fas Δ 5 Δ 6, Fas Δ 4 Δ 6 and Fas Δ 4 Δ 5 Δ 6 transcripts observed in the lymphoid tumour cell lines. Three bands detected in the PBMC sample from cat 2 were shown to correspond to Fas Δ 6, Fas Δ 5 Δ 6 and Fas Δ 4 Δ 6 transcripts. These results indicate that some splicing variants of feline Fas mRNA are also present in Con A-activated normal feline PBMCs.

Detection of Fas mRNA variants in primary tumour tissues from cats with spontaneous lymphoma

To investigate the significance of the alternatively spliced variants of Fas mRNA in feline lymphoma, we examined the presence of the splicing variants in primary tumour tissues from cats with naturally occurring lymphoma. We

used primary tumour tissues from 11 cats with lymphoma of different forms, such as thymic, multicentric and alimentary forms. Fas mRNA was detected in seven of the 11 lymphoma samples by RT-PCR, whereas β -actin, as an internal control, was amplified to a similar level in all the samples. In the seven samples containing Fas mRNA, RT-PCR with two primer pairs (6S/6R and 8S/8R) generated bands derived from the authentic Fas gene transcript, but RT-PCR with 7S/7R primers gave various splicing variants (Fig. 2c).

All of the bands detected by RT-PCR were sequenced and their sequences were compared with those of authentic and alternatively spliced feline Fas mRNA-derived cDNAs. In cases 4 and 7, a band derived from the authentic Fas mRNA (band A) was the most intense as compared with other bands, but in other cases, it was faint (cases 2 and 3) or absent (cases 1, 5 and 6). In case 7, in addition to the band of authentic transcript (band A), RT-PCR generated all of the five spliced variants of Fas Δ 6 (band B), Fas Δ 4 (band C), Fas Δ 5 Δ 6 (band D), Fas Δ 4 Δ 6 (band E) and Fas Δ 4 Δ 5 Δ 6 (band F) transcripts.

Discussion

The presence of several transcript variants of the human Fas gene has been reported previously (Cascino *et al.*, 1995; Liu *et al.*, 1995; Schumann *et al.*, 1997). In the cell lines from lymphoma, leukaemia and other tumours in humans, five Fas mRNA variants, which lacked exon 6, exon 4, exons 4 and 6, exons 3 and 4, and exons 3, 4 and 6, were reported (Cascino *et al.*, 1995; Papoff *et al.*, 1996). In addition to these variants, another isoform (lacking exons 4 and 7) was detected in human ventricular myocardium (Schumann *et al.*, 1997). These Fas mRNA variants were shown to be generated by alternative splicing and to lack the transmembrane domain because of the absence of exon 6 or its frameshift. In another report, a Fas mRNA variant, lacking exon 8, which contains the death domain, was found in human lymphoma cell lines resistant to apoptosis (Cascino *et al.*, 1996). In this study, we detected five splicing variants of feline Fas mRNA lacking exon 4, exon 6, exons 5 and 6, exons 4 and 6, and exons 4, 5, and 6 in feline lymphoid tumour cell lines. Of these alternatively spliced variants of Fas mRNA, those lacking exons 5 and 6, and exons 4, 5, and 6, shown in this study, have not been detected previously. As all of these splicing variants of Fas mRNA identified in this study were shown to encode Fas proteins lacking a transmembrane domain, they might be translated to soluble proteins, as reported in human and murine Fas conceivably associated with the pathogenesis of various diseases such as tumours and autoimmune diseases. Unfortunately, the presence of the soluble Fas protein could not be identified in the cat system because monoclonal antibodies directed to human and murine Fas did not cross-react with feline Fas and anti-feline Fas immunoglobulin was not available.

A mechanism for the alternative splicing, mentioned above, is called exon skipping. Meanwhile, in mice,

abnormal splicing of the Fas gene, owing to insertions of some unrelated exons, has also been reported (Adachi *et al.*, 1993; Kobayashi *et al.*, 1993; Chu *et al.*, 1993; Wu *et al.*, 1993). It has been shown that *lpr* mice cannot express normal functional membrane-bound Fas, and this results in generalized lymphadenopathy and autoimmune disease (Kobayashi *et al.*, 1993). *lpr* mice were shown to have an insertion of the Etn transposon between exon 2 and exon 3 of the Fas gene, producing a truncated, deficient form of Fas. Of the mRNA variants of the feline Fas gene detected in this study, there was no variant mRNA as a result of such insertion of unrelated exons.

In human PBMCs, the expression of Fas and its splicing variants was detected, even in the absence of mitogen stimulation (Cheng *et al.*, 1994). Stimulation of human PBMCs with phytohaemagglutinin was shown to increase the amount of authentic Fas mRNA and decrease that of its splicing variants (Liu *et al.* 1995). In contrast, we were unable to detect Fas mRNA in unstimulated feline PBMCs, but observed the distinct expression of Fas mRNAs (including its authentic transcript and splicing variants in PBMCs) after Con A stimulation. A band derived from the authentic transcript was more intense than other bands derived from splicing variants in Con A-activated feline PBMCs. Therefore, in feline PBMCs, unlike human PBMCs, Con A stimulation was considered to enhance the expression of authentic and variant Fas mRNAs.

In this study, we detected alternatively spliced variants of Fas mRNA in primary tumour cells from naturally occurring feline lymphomas, as well as in feline lymphoma cell lines. A splicing variant of Fas mRNA lacking exon 6 has been often detected in various malignancies, such as leukaemias (Sugahara *et al.*, 1997; Kamihira *et al.*, 1999; Inaba *et al.*, 1999) and carcinomas (Mizutani *et al.*, 1998; Kimura *et al.*, 1999; Ueno *et al.*, 1999; Nonomura *et al.*, 2000), in humans, but no other splicing variant of the Fas gene has been identified in primary neoplastic tissues and cells in humans. In the present study, various splicing variants of Fas mRNA lacking exon 4, exon 6, exons 5 and 6, exons 4 and 6, and exons 4, 5 and 6 were observed, even in the absence of authentic Fas transcript in feline primary lymphoma cells. Several reports have indicated that the amount of soluble Fas in serum is correlated with the clinical parameters and the degree of malignancy in adult T-cell leukaemia patients (Sugahara *et al.*, 1997; Kamihira *et al.*, 1999); however, we were unable to establish a relationship between the Fas mRNA pattern of the splicing variants and the clinical prognosis of lymphoma. An *in situ* RT-PCR study revealed the presence of normal Fas and soluble Fas in samples from gastric adenocarcinoma and its metastatic lymph node (Lee *et al.*, 1998). In these reports, on human malignancies, the amounts of variant and normal Fas transcripts were shown to be proportional to those of membrane-bound and soluble Fas proteins, respectively. Although, in this study, we were unable to measure the amount of soluble Fas protein in cats with lymphoma, Fas proteins lacking the transmembrane domain derived from

the alternatively spliced mRNAs may exist as soluble forms in the sera of these cats.

A variety of alternatively spliced variants of Fas mRNA were detected in feline lymphoid cells in this study. The alternatively spliced variants identified in this study, and the putative resultant soluble forms of Fas, may be associated with the pathogenesis of tumours, autoimmune diseases, and several other diseases in cats. Further studies are required to establish an assay system to measure the level of soluble Fas protein in cats and to investigate the role of soluble Fas in pathogenesis.

Acknowledgements

This study was supported by grants from the Japan Health Science Foundation, Ministry of Education, Science, Sports and Culture, Recombinant Cytokine Project, provided by the Ministry of Agriculture, Forestry and Fisheries, Japan (RCP1988-3110).

References

- Adachi, M., Watanabe-Fukunaga, R. & Nagata, S. (1993) Aberrant transcription caused by the insertion of an early transposable element in an intron of the Fas antigen gene of *lpr* mice. *Proceedings of the National Academy of Sciences of the USA*, **90**, 1756.
- Behrmann, I., Walczak, H. & Krammer, P.H. (1994) Structure of the human APO-1 gene. *European Journal of Immunology*, **24**, 3057.
- Breathnach, R., Benoist, C., O'Hare, K., Gannon, F. & Chambon, P. (1978) Ovalbumin gene: evidence for a leader sequence in mRNA and DNA sequences at the exon-intron boundaries. *Proceedings of the National Academy of Sciences of the USA*, **75**, 4853.
- Cascino, I., Fiucci, G., Papoff, G. & Ruberti, G. (1995) Three functional soluble forms of the human apoptosis-inducing Fas molecule are produced by alternative splicing. *Journal of Immunology*, **154**, 2706.
- Cascino, I., Papoff, G., De Maria, R., Testi, R. & Ruberti, G. (1996) Fas/Apo-1 (CD95) receptor lacking the intracytoplasmic signaling domain protects tumor cells from Fas-mediated apoptosis. *Journal of Immunology*, **156**, 13.
- Cheney, C.M., Rojko, J.L., Kociba, G.J., Wellman, M.L., Di Bartola, S.P., Rezanka, L.J., Forman, L. & Mathes, L.E. (1990) A feline large granular lymphoma and its derived cell line. *In Vitro Cell and Developmental Biology*, **26**, 455.
- Cheng, J., Liu, C., Koopman, W.J. & Mountz, J.D. (1995) Characterization of human Fas gene. Exon/intron organization and promoter region. *Journal of Immunology*, **154**, 1239.
- Cheng, J., Zhou, T., Liu, C., Shapiro, J.P., Brauer, M.J., Kiefer, M.C., Barr, P.J. & Mountz, J.D. (1994) Protection from Fas-mediated apoptosis by a soluble form of the Fas molecule. *Science*, **263**, 1759.
- Chu, J.L., Drappa, J., Parnassa, A. & Elkon, K.B. (1993) The defect in Fas mRNA expression in *MRL/lpr* mice is associated with insertion of the retrotransposon, ETn. *Journal of Experimental Medicine*, **178**, 723.
- Hara, T., Tsurumi, H., Takemura, M., Goto, H., Yamada, T., Sawada, M., Takahashi, T. & Moriwaki, H. (2000) Serum-soluble fas level determines clinical symptoms and outcome of patients with aggressive non-Hodgkin's lymphoma. *American Journal of Hematology*, **64**, 257.
- Hasunuma, T., Kayagaki, N., Asahara, H., Motokawa, S., Kobata, T., Yagita, H., Aono, H., Sumida, T., Okumura, K. & Nishioka, K. (1997) Accumulation of soluble Fas in inflamed joints of patients with rheumatoid arthritis. *Arthritis and Rheumatism*, **40**, 80.
- Inaba, H., Komada, Y., Li, Q.S., Zhang, X.L., Tanaka, S., Azuma, E., Yamamoto, H. & Sakurai, M. (1999) mRNA expression of variant Fas molecules in acute leukemia cells. *American Journal of Hematology*, **62**, 150.
- Itoh, N., Yonehara, S., Ishii, A., Yonehara, M., Mizushima, S., Sameshima, M., Hase, A., Seto, Y. & Nagata, S. (1991) The polypeptide encoded by the cDNA for human cell surface antigen Fas can mediate apoptosis. *Cell*, **66**, 233.
- Kamihira, S., Yamada, Y., Tomonaga, M., Sugahara, K. & Tsuruda, K. (1999) Discrepant expression of membrane and soluble isoforms of Fas (CD95/APO-1) in adult T-cell leukaemia: soluble Fas isoform is an independent risk factor for prognosis. *British Journal of Haematology*, **107**, 851.
- Kimura, M., Tomita, Y., Imai, T., Saito, T., Katagiri, A., Tanikawa, T., Takeda, M. & Takahashi, K. (1999) Significance of serum-soluble CD95 (Fas/APO-1) on prognosis in renal cell cancer patients. *British Journal of Cancer*, **80**, 1648.
- Kobayashi, S., Hirano, T., Kakinuma, M. & Uede, T. (1993) Transcriptional repression and differential splicing of Fas mRNA by early transposon (ETn) insertion in autoimmune *lpr* mice. *Biochemistry and Biophysics Research Communications*, **191**, 617.
- Lee, S.H., Kim, S.Y., Lee, J.Y., Shin, M.S., Dong, S.M., Na, E.Y. *et al.* (1998) Detection of soluble Fas mRNA using in situ reverse transcription-polymerase chain reaction. *Laboratory Investigations*, **78**, 453.
- Liu, C., Cheng, J. & Mountz, J.D. (1995) Differential expression of human Fas mRNA species upon peripheral blood mononuclear cell activation. *Biochemistry Journal*, **310**, 957.
- Miura, T., Shibuya, M., Tsujimoto, H., Fukasawa, M. & Hayami, M. (1989) Molecular cloning of a feline leukemia provirus integrated adjacent to the C-myc gene in a feline T-cell leukemia cell line and the unique structure of its long terminal repeat. *Virology*, **169**, 458.
- Miura, T., Tsujimoto, H., Fukasawa, M., Kodama, T., Shibuya, M., Hasegawa, A. & Hayami, M. (1987) Structural abnormality and over-expression of the myc gene in feline leukemias. *International Journal of Cancer*, **40**, 564.
- Mizuno, T., Endo, Y., Momoi, Y., Goto, Y., Nishimura, Y., Tsubota, K. *et al.* (1998) Molecular cloning of feline Fas antigen and Fas ligand cDNAs. *Veterinary Immunology and Immunopathology*, **65**, 161.
- Mizutani, Y., Yoshida, O. & Bonavida, B. (1998) Prognostic significance of soluble Fas in the serum of patients with bladder cancer. *Journal of Urology*, **160**, 571.
- Nagata, S. (1997) Apoptosis by death factor. *Cell*, **88**, 355.
- Niitsu, N., Sasaki, K. & Umeda, M. (1999) A high serum soluble Fas/APO-1 level is associated with a poor outcome of aggressive non-Hodgkin's lymphoma. *Leukemia*, **13**, 1434.
- Nonomura, N., Nishimura, K., Ono, Y., Fukui, T., Harada, Y., Takaha, N., Takahara, S. & Okuyama, A. (2000) Soluble Fas in serum from patients with renal cell carcinoma. *Urology*, **55**, 151.
- Papoff, G., Cascino, I., Eramo, A., Starace, G., Lynch, D.H. & Ruberti, G. (1996) An N-terminal domain shared by Fas/Apo-1 (CD95) soluble variants prevents cell death *in vitro*. *Journal of Immunology*, **156**, 4622.
- Rickard, C.G., Post, J.E., Noronha, F. & Barr, L.M. (1969) A transmissible virus-induced lymphocytic leukemia of the cat. *Journal of the National Cancer Institute*, **42**, 987.
- Schumann, H., Morawietz, H., Hakim, K., Zerkowski, H.R., Eschenhagen, T., Holtz, J. & Darmer, D. (1997) Alternative splicing of the primary Fas transcript generating soluble Fas antagonists is suppressed in the failing human ventricular myocardium. *Biochemistry and Biophysics Research Communications*, **239**, 794.
- Snyder, H.W., Jr, Hardy W.D., Jr, Zuckerman E.E. & Fleissner E. (1978) Characterisation of a tumour-specific antigen on the surface of feline lymphosarcoma cells. *Nature*, **275**, 656.

- Sugahara, K., Yamada, Y., Hiragata, Y., Matsuo, Y., Tsuruda, K., Tomonaga, M., Maeda, T., Atogami, S., Tsukasaki, K. & Kamihira, S. (1997) Soluble and membrane isoforms of Fas/CD95 in fresh adult T-cell leukemia (ATL) cells and ATL-cell lines. *International Journal of Cancer*, **72**, 128.
- Theilen, G.H., Kawakami, T.G., Rush, J.D. & Munn, R.J. (1969) Replication of cat leukemia virus in cell suspension cultures. *Nature*, **222**, 589.
- Ueno, T., Toi, M. & Tominaga, T. (1999) Circulating soluble Fas concentration in breast cancer patients. *Clinical Cancer Research*, **5**, 3529.
- Wu, J., Zhou, T., He, J. & Mountz, J.D. (1993) Autoimmune disease in mice due to integration of an endogenous retrovirus in an apoptosis gene. *Journal of Experimental Medicine*, **178**, 461.
- Yoo, J., Stone, R.T., Kappes, S.M., Toldo, S.S., Fries, R. & Beattie, C.W. (1996) Genomic organization and chromosomal mapping of the bovine Fas/APO-1 gene. *DNA Cell Biology*, **15**, 377.
- Yufu, Y., Choi, I., Hirase, N., Tokoro, A., Noguchi, Y., Goto, T., Uike, N. & Kozuru, M. (1998) Soluble Fas in the serum of patients with non-Hodgkin's lymphoma: higher concentrations in angioimmunoblastic T-cell lymphoma. *American Journal of Hematology*, **58**, 334.



Expression of apoptosis-related gene mRNAs in feline T-cells infected with feline immunodeficiency virus (FIV)

Junpei Yamazaki^a, Nami Hasebe^a, Shunpei Nagafuchi^a, Kenji Baba^b,
Hajime Tsujimoto^b, Rui Kano^{a,*}, Atsuhiko Hasegawa^a

^a Department of Pathobiology, Nihon University School of Veterinary Medicine, 1866 Kameino, Fujisawa, Kanagawa 252-8510, Japan

^b Department of Veterinary Internal Medicine, Graduate School of Agricultural and Life Sciences, The University of Tokyo, 1-1-1 Yayoi, Bunkyo, Tokyo 113-8657, Japan

Received 26 June 2003; received in revised form 27 February 2004; accepted 14 March 2004

Abstract

In the present study, full length of feline *bax*, *bcl-2*, *bcl-xL* and *caspase 3* genes were sequenced and the expression of these mRNAs were also investigated in FIV-infected lymphocytes.

The full length cDNA sequence of *bax* (646 bp), *bcl-2* (1423 bp), *bcl-xL* (1163 bp) and *caspase 3* genes (1208 bp) contained a single open reading frame of 579 bp coding 193 amino acids, 708 bp coding 236 amino acids, 702 bp coding 234 amino acids and 834 bp coding 278 amino acids, respectively.

Number of apoptotic Kumi-1 cells gradually increased after FIV infection and approximately 70% were apoptotic and 30% were viable in the cells infected with FIV after 8-day incubation, though approximately 80% were non-apoptotic and 20% were dead in non-infected cells.

The expression of *bcl-2* mRNA in lymphocytes of established cell line was increased by FIV. The amounts of mRNAs of *bax*, *caspase 3* and *bcl-xL* in FIV-infected cells were not different from those in uninfected control cells.

© 2004 Elsevier B.V. All rights reserved.

Keywords: *bcl-2*; *bax*; *bcl-xL*; *Caspase 3*; Feline immunodeficiency virus

1. Introduction

Feline immunodeficiency virus (FIV) is a lentivirus and associated with slow progressive disease in domestic cats. FIV replicates in T-lymphocytes (CD4⁺ cells and CD8⁺ cells), B-lymphocytes, macrophages, and astrocytes (Sellon, 1998). The hallmark of FIV pathogenesis is the progressive disruption of normal

immune function, the mechanisms of which are under intense investigation. Within months to years after infection, an immune deficiency stage similar to acquired immunodeficiency syndrome (AIDS) in humans develops. Therefore, the FIV infection has been studied as a model for study of HIV infection.

Early immunologic abnormalities after spontaneous and experimental infection are decreases of CD4⁺ cells in total number and relative proportion. CD4⁺/CD8⁺ ratios were not different extremely in FIV-infected cats between with and without clinical signs, though loss of CD4⁺ cells leads to inversion

* Corresponding author. Tel.: +81-466-84-3649;
fax: +81-466-84-3649.

E-mail address: kano@brs.nihon-u.ac.jp (R. Kano).

of the CD4⁺/CD8⁺ ratio in humans with HIV infection. The decrease of CD4⁺ cells could include the decreased production secondary to bone marrow or thymic damage due to the infection, lysis of infected cells induced by FIV itself (cytopathic effects), destruction of infected cells by the immune system, and induction of cell death by apoptosis. Apoptosis induced by Fas ligand (L) and TNF- α was reported in FIV-infected lymphocytes (Ohno et al., 1994; Mizuno et al., 1997; Mizuno et al., 1998). Tompkins et al. (2002) reported that flow cytometry revealed high percentages of CD8⁺ and CD4⁺ cells expressing B7.1 + B7.2 CTLA4 + T cells and that apoptosis occurred in these cells in lymph node. The B7.1 and B7.2 costimulatory molecules on antigen-presenting cells provide second signals for regulating T-cell immune responses via CD28 and cytotoxic T-lymphocyte antigen 4 (CTLA4) on T-cells.

On the other hand, cells obtained from HIV-infected patients and cells infected with HIV in vitro were deviated in the regulation of Fas and FasL expression. Acute HIV infection of the promonocytic cell line U937 is associated with viral replication-dependent apoptosis that is characterized by the increased membrane expression of Fas and FasL, by the down-regulation of antiapoptotic proteins, *Bcl-2* and *Bcl-xL*, and by concomitant increase in proapoptotic proteins, *Bcl-xS* and *Bax* (Badley et al., 2000). Interestingly, though the expression of *Bax*, *Bcl-xL*, and *Bcl-xS* in cells infected with HIV does not differ from that of uninfected controls, the expression of *Bcl-2* was increased in T-cells from HIV-infected patients. (Badley et al., 2000).

However, the precise molecular mechanism of apoptosis in FIV-infected lymphocytes is unknown at present. In the present study, full length sequences of feline *bax*, *bcl-2*, *bcl-xL* and *caspase 3* genes were sequenced and their expression of mRNAs were also investigated in FIV-infected lymphocytes.

2. Materials and methods

2.1. Preparation of cDNA for feline *bax*, *bcl-2*, *bcl-xL* and *caspase 3* genes

The feline T-lymphocyte cell line of FT-1 (Miura et al., 1987, 1989) was cultured in Dulbecco's mod-

ified eagle medium supplemented with 5% fetal calf serum. Total RNA was extracted from 5×10^6 cells with RNeasy total RNA kit (QIAGEN, CA, USA). Reverse transcription of the poly(A)⁺ RNA was performed with a OmniscriptTM Reverse Transcriptase kit (QIAGEN).

A series of 5'- and 3'-RACE-PCR experiments were carried out to determine the full length cDNA sequence of the feline *bax*, *bcl-2*, *bcl-xL* and *caspase 3* genes. The sequences of gene-specific primers were designed from the sequence of the conserved region in *bax*, *bcl-2*, *bcl-xL* and *caspase 3* genes of human and mouse, respectively (Table 1).

The 5'- and 3'-sides of each gene were determined, respectively, according to the user manuals of 5'-RACE system for rapid amplification of cDNA ends (GIBCOBRL, MD, USA) and 3'-RACE system for rapid amplification of cDNA ends (GIBCOBRL). The PCR products of 5'- and 3'-sides of each gene were sequenced by dideoxy chain termination method using an ABI PRISM 310 Genetic Analyzer (ABI Prism, Foster City, USA).

2.2. Preparation of cDNA from FIV-infected feline T-lymphocyte cell line and determination of the viability and apoptosis rate

FIV inoculation was performed by a previous report (Mizuno et al., 2003). The feline T-lymphocyte cell line of Kumi-1 (Hohdatsu et al., 1996) was cultured in RPMI1640 medium supplemented with 5% fetal calf serum, 100 U/ml of human recombinant IL-2 and 50 μ mol of 2-mercaptoethanol. Kumi-1 cells were inoculated with FIV of Sendai-1 strain (Hohdatsu et al., 1996) (500 cpm/ml per 1×10^6). After adsorption for 2 h at 37 °C, the cells were washed in RPMI1640 medium three times and resuspended to a final concentration of 5×10^5 cells/ml.

Three, six, and eight days after infection, the cells were harvested to measure the viable cell counts with trypan blue stain and to confirm apoptosis with TUNEL assay. The TUNEL assay was performed using DeadEnd colorimetric apoptosis detection system, following the manufacturer's instructions (Promega Corporation, Madison, USA) (Oguma et al., 2000). Total RNA was extracted from cells at each day with RNeasy total RNA kit (QIAGEN, CA, USA). Reverse transcription of the poly(A)⁺ RNA was per-

Table 1
PCR primers, annealing temperature and amplified fragment size for real-time PCR

Gene	Sequence	Annealing temperature (amplified fragment size)
<i>bax</i>		
Sense	5'-CCAGCTCTGAGCAGATCAT-3'	65 °C (212 bp)
Reverse	5'-CACTCCC GCCACAAAGATGG-3'	
<i>bcl-2</i>		
Sense	5'-GGAGGATTGTGGCCTTCT-3'	65 °C (223 bp)
Reverse	5'-GTTATCCTGGATCCAGGTGT-3'	
<i>bcl-xL</i>		
Sense	5'-CTTGGATGGCCACTTACCTGA-3'	58 °C (278 bp)
Reverse	5'-TCTTCTGGTCAITTCGACTGAAG-3'	
<i>caspase 3</i>		
Sense	5'-AGCCATGGTGAAGAAGAA-3'	65 °C (208 bp)
Reverse	5'-TGTTGCCACCTTTCGGTT-3'	
GAPDH		
Sense	5'-TGGTGAAGCAGGCATCAGAG-3'	60 °C (157 bp)
Reverse	5'-CAGGAAATGAGCTTGACAAAGTGG-3'	

formed with a Omniscript™ Reverse Transcriptase kit (QIAGEN).

2.3. Real-time PCR

The quantification of *bax*, *bcl-2*, *bcl-xL* and *caspase 3* transcripts in FIV-infected lymphocytes was carried out with the LightCycler PCR system (Roche Diagnostics, Meylan, France) using the DNA binding SYBR Green I dye for the detection of PCR products. The feline glyceraldehyde-3-phosphate dehydrogenase (GAPDH) (Harley et al., 1999) gene was used as reference for mRNA expression. Quantities of each gene and GAPDH transcripts were determined by comparison to a DNA external standard. The forward and reverse-specific primer sequences used, the size of the amplified fragment and the annealing temperature were listed in Table 1.

DNA standards were prepared from PCR using cDNA of cells. The amount of extracted DNA was quantified by spectrophotometry and expressed as copy number. A serial dilution was used to generate each standard curve. After 2 min of denaturation at 95 °C, the reaction were cycled 40 times for 5 s at 95 °C, 10 s at the annealing temperature, and 15 s at 72 °C. Product specificity was determined by melting curve analysis as described in the LightCycler handbook. We used feline GAPDH gene as a RT-PCR

control (Harley et al., 1999). The amounts of transcripts in each sample is given as copy number. The results are expressed as ratios of each transcript to GAPDH transcripts.

3. Results

3.1. Full length sequences of feline *bax*, *bcl-2*, *bcl-xL* and *caspase 3* cDNAs

Using cDNA of FT-1 cells as a template, full length sequences of feline *bax*, *bcl-2*, *bcl-xL* and *caspase 3* genes were cloned using 5'- and 3'-RACE methods.

The full length cDNA sequence of the *bax* gene (646 bp) contained a single open reading frame of 579 bp coding 193 amino acids (Fig. 1). The sequence was deposited in the DDBJ database (accession no. AB080724, feline *bax* gene, complete cds).

The amino acid sequence of feline *bax* shared 98–92% sequence identity with the human (GenBank accession no. L22473) and the mouse (L22472) *bax* genes (Fig. 1).

The full length cDNA sequence of the *bcl-2* gene (1423 bp) contained a single open reading frame of 708 bp coding 236 amino acids (Fig. 2). The sequence was deposited in the DDBJ database (accession no. AB096611, feline *bcl-2* gene, complete cds).

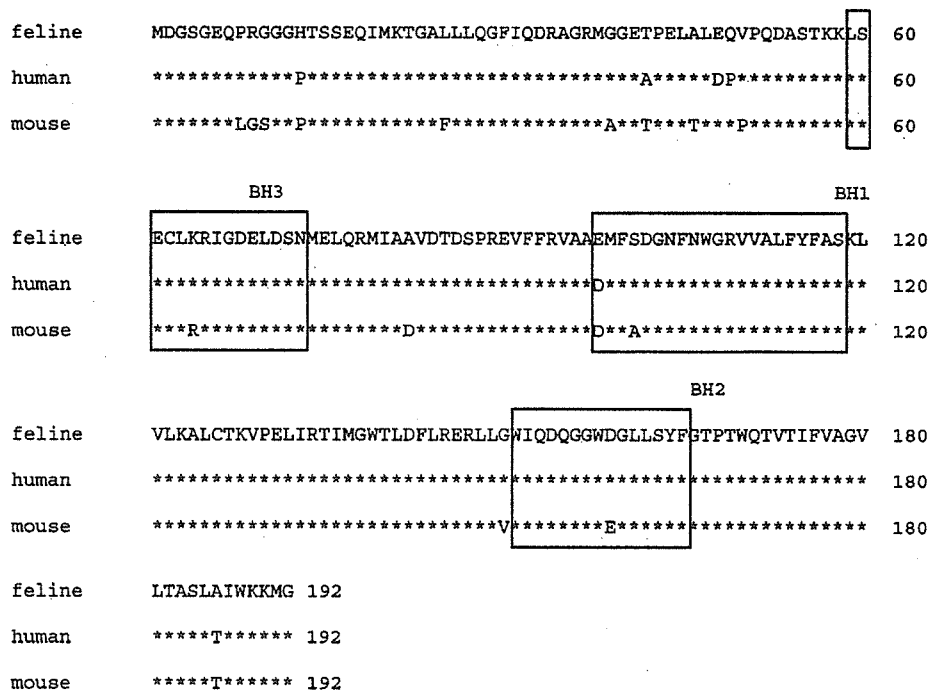


Fig. 1. Comparison of homologous regions of the predicted protein sequences of *bax* among feline, human (L22473) and mouse (L22472). Asterisk indicates identity with the amino acids of the feline *bax*. BH1–3 indicate *Bcl-2* homology domain 1–3, respectively.

The amino acid sequence of feline *bcl-2* shared 90–86% sequence identity with the human (GenBank accession no. M14745) and the mouse (M16506) *bcl-2* genes (Fig. 2).

The full length cDNA sequence of the *bcl-xL* gene (1163 bp) contained a single open reading frame of 702 bp coding 234 amino acids (Fig. 3). The sequence was deposited in the DDBJ database (ac-

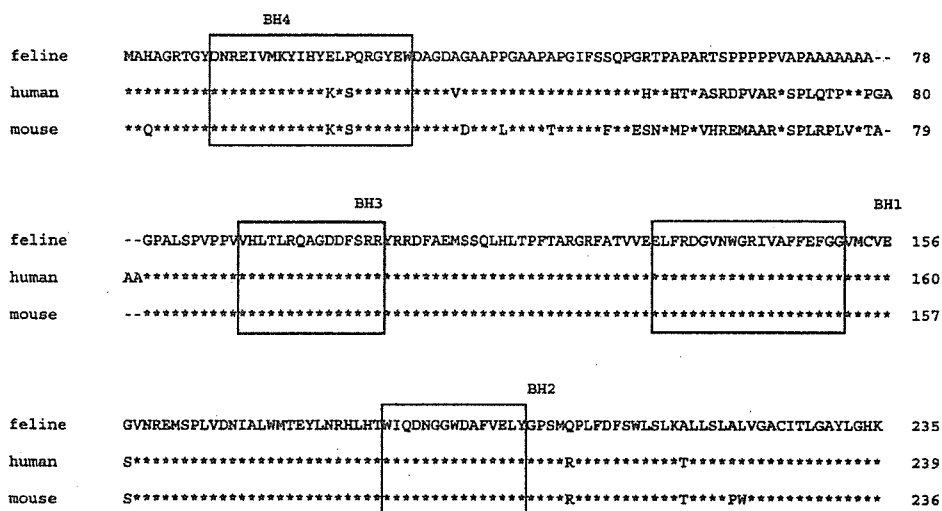


Fig. 2. Comparison of homologous regions of the predicted protein sequences of *bcl-2* among feline, human (M14745) and mouse (M16506). Asterisk indicates identity with the amino acids of the feline *bcl-2*. BH1–4 indicate *Bcl-2* homology domain 1–4, respectively.



Fig. 3. Comparison of homologous regions of the predicted protein sequences of *bcl-xL* among feline, human (Z23115) and mouse (U51278). Asterisk indicates identity with the amino acids of the feline *bcl-xL*. BH1-4 indicate *Bcl-2* homology domain 1-4, respectively.

cession no. AB080951, feline *bcl-xL* gene, complete cds).

The amino acid sequence of feline *bcl-xL* shared 99-96% sequence identity with the human (GenBank accession no. Z23115) and the mouse (U51278) *bcl-xL* genes (Fig. 3).

The full length cDNA sequence of the *caspase 3* gene (1208 bp) contained a single open reading frame

of 834 bp coding 278 amino acids (Fig. 4). The sequence was deposited in the DDBJ database (accession no. AB090246, feline *caspase 3* gene, complete cds).

The amino acid sequence of feline *caspase 3* shared 87-87% sequence identity with the human (GenBank accession no. AY219866) and the mouse (Y13086) *caspase 3* genes (Fig. 4).

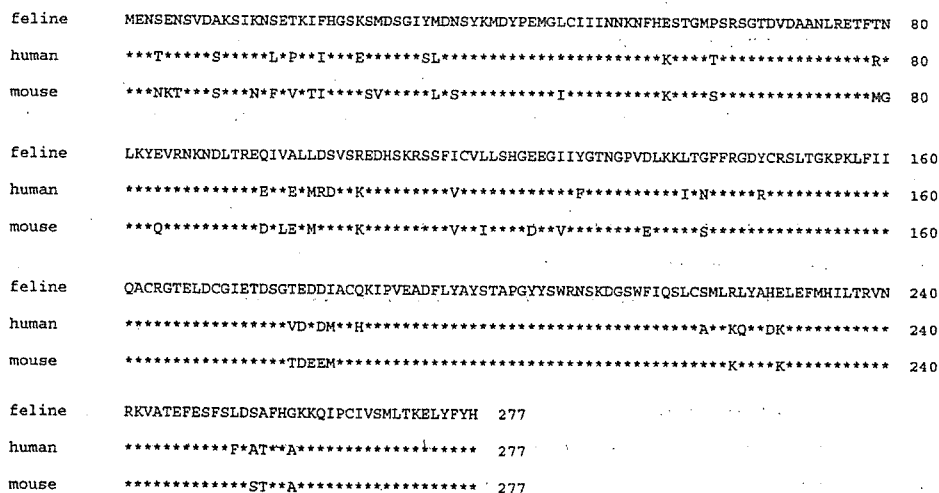


Fig. 4. Comparison of homologous regions of the predicted protein sequences of *caspase 3* among feline, human (AY219866) and mouse (Y13086). Asterisk indicates identity with the amino acids of the feline *caspase 3*.

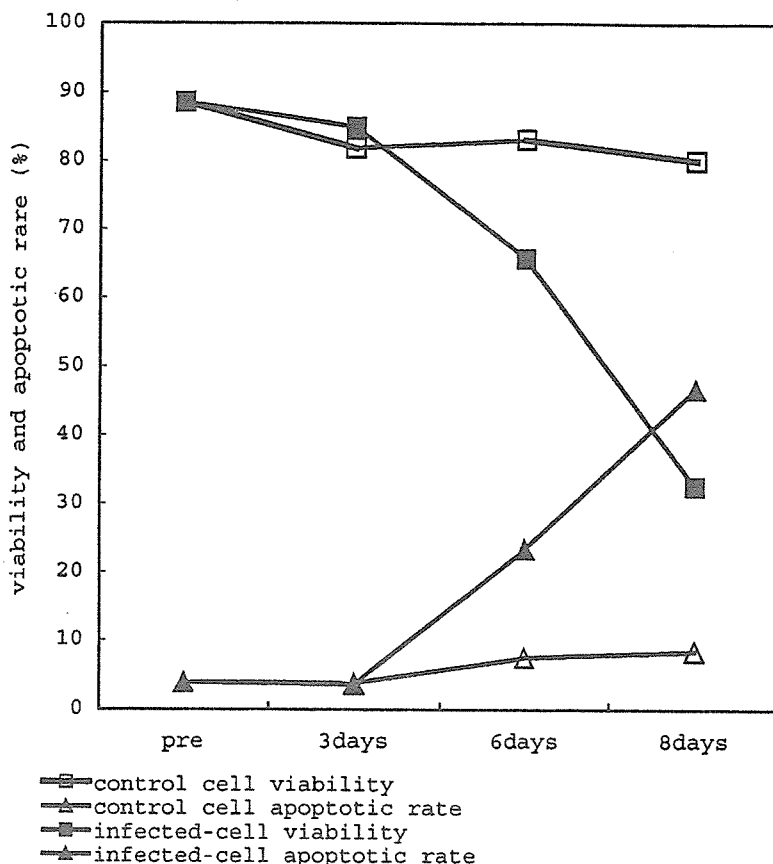


Fig. 5. The viability and apoptotic rate of infected cells and control cells. Apoptotic Kumi-1 cells gradually increased after FIV infection. Approximately 70% had been apoptotic and 30% were viable in the cells infected with FIV but approximately 80% were non-apoptotic and 20% had been dead in non-infected cells after 8-day incubation.

3.2. The viability and apoptosis rate in FIV-infected cells

Apoptotic Kumi-1 cells gradually increased after FIV infection (Fig. 5). Approximately 70% cells had been apoptotic and 30% were viable in the cells infected with FIV while incubation after 8 days approximately and 20% had been dead 80% were non-apoptotic in non-infected control cells.

3.3. Analysis of *bax*, *bcl-2*, *bcl-xL* and *caspase 3* gene mRNAs by real-time PCR

By real-time PCR analysis, *bax*, *bcl-2*, *bcl-xL* and *caspase 3* gene mRNAs were detectable in lympho-

cytes pre- and post-FIV infection (Fig. 6a–d). Although the expression of *bcl-2* mRNA was increased in FIV-infected cells, mRNAs of *bax*, *caspase 3* and *bcl-xL* were expressed in the infected cells as in the non-infected control cells (Fig. 6a–d).

4. Discussion

In the present study, full length sequences of feline *bax*, *bcl-2*, *bcl-xL* and *caspase 3* genes were sequenced and their expression of mRNAs were also investigated in FIV-infected lymphocytes.

The amino acid sequences of feline *bax*, *bcl-2*, *bcl-xL* and *caspase 3* genes were highly conserved in comparison with those of human and mouse, respec-

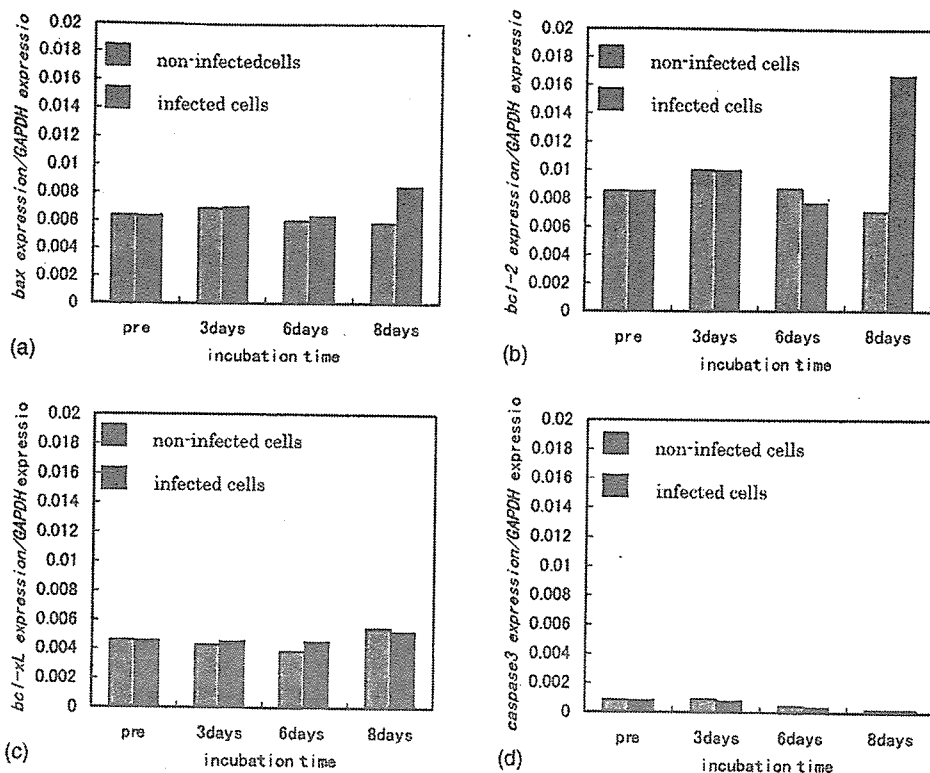


Fig. 6. Quantification of (a) *bax*, (b) *bcl-2*, (c) *bcl-xL* and (d) *caspase 3* mRNAs by LightCycler after infection by FIV for 0, 3, 6, and 8 days. The results are expressed as ratios (Y-axis) of each transcripts to GAPDH transcripts. The black and gray columns indicate the expression in infected cells and non-infected cells, respectively.

tively, suggesting that these feline genes might play similar roles to human and mouse genes.

Approximately 70% were apoptotic and the other 30% were viable in the cells infected with FIV, though the approximately 80% were non-apoptotic and 20% were dead in non-infected cells after 8-day incubation (Fig. 5). The expression of *bcl-2* mRNA was increased in FIV-infected cells after 8-day incubation (Fig. 6b), indicating the correlation between expression of *bcl-2* and viral replication in lymphocyte culture. The increased expression of antiapoptotic gene of *bcl-2* in FIV-infected cells, as in T-cells from HIV-infected patients (Sandstrom et al., 1996) might play some antiapoptotic role in FIV-infected cells. The expression of *bcl-2* was reported to associate with enhanced HIV replication in infected cells (Sandstrom et al., 1996). Tat protein of HIV was proved to stimulate the *bcl-2* mRNA and *Bcl-2* protein expression in HIV-infected T-cell line (Zauli et al., 1995), suggesting that tat might

be a promotor for *bcl-2* mRNA expression to inhibit host cell apoptosis (Zauli et al., 1995). Tat gene was also confirmed to be in FIV genome and related with virus replication in host cells (de Parseval and Elder, 1999). Therefore, FIV tat might also stimulate the expression of *bcl-2* mRNA in infected feline T-cells.

Apoptotic cells in FIV-infected Kumi-1 cells increased progressively, indicating that FIV infection-induced cell death in these cells. Therefore, amount of apoptosis induction genes such as *bax* and *caspase 3* mRNAs was expected to increase in FIV-infected cells. However, the expression of *bax* and *caspase 3* genes in the infected cells did not differ from that in non-infected control cells. The results were consistent to the expression of apoptosis induction genes in T-cells from HIV-infected patients (Badley et al., 2000). Therefore, another apoptosis inducible mechanisms such as ceramide might be concerned in FIV- and HIV-infected cells.